Reprinted from April 1991, Vol. 113, Journal of Vibration and Acoustics

Prediction of Low Frequency Vibrational Frequencies of Submerged Structures

G. C. Everstine
Applied Mathematics Division (184),
David Taylor Research Center,
Bethesda, MD 20084

Practical numerical techniques are described for calculating the low frequency vibrational resonances of general submerged structures. Both finite element and boundary element approaches for calculating fully-coupled added mass matrices are presented and illustrated. The finite element approach is implemented using existing structural analysis capability in NASTRAN. The boundary element approach uses the NASHUA structural acoustics program in combination with NASTRAN to compute the added mass matrix. The two procedures are compared in application to a submerged cylindrical shell with flat end closures. Both procedures proved capable of computing accurate submerged resonances; the more elegant boundary element procedure is easier to use but may be more expensive computationally.

Introduction

One problem of interest in numerical structural acoustics is that of determining the natural vibrational frequenices of general submerged structures. At low frequencies, the fluid appears to the structure like an added mass (Geers, 1971), i.e., the fluid pressure on the wet surface is in phase with structural acceleration. At higher frequencies, the fluid impedance (the ratio of fluid pressure to velocity) is mathematicaly complex, since it involves both mass-like and damping-like effects. The primary difference between these two situations from a computational point of view is that the low frequency calculation can be performed using standard real eigenvalue analysis techniques, whereas the higher frequency calculation requires more expensive complex eigenanalysis. In addition, as frequency increases, the added mass effects diminish and the damping (or piston) effects increase, so that the interpretation of the complex eigenvectors as "normal modes" becomes more difficult. For shell structures, these complications become somewhat academic, since shells have high modal density above the first few modes, making the usefulness of computing such modes in doubt.

Consequently, for this paper, interest is restricted to the calculation of low frequency modes, in which case the finite element calculation of submerged resonances reduces to that of computing the added mass effects of the surrounding fluid on the structure. Since, in general, the vibrational modes of a submerged structure are different from the structure's in-vacuo modes, a fully-coupled calculation is required.

The added mass calculation requires solving Laplace's equation in the fluid domain exterior to the structure, a calculation which can be performed using either finite element or boundary element techniques, among others. This paper describes the computation of submerged natural frequencies using both approaches. It starts by summarizing the relevant theory and then illustrates the two approaches using as an example the vibrations of a submerged cylindrical shell with flat end closures.

Contributed by the Technical Committee on Vibration and Sound for publication in the JOURNAL OF VIBRATION AND ACOUSTICS. Manuscript received January 1990; revised April 1990

Theoretical Approaches

Consider an arbitrary three-dimensional elastic structure submerged in a heavy fluid like water. The structure is modeled mathematically using the equations of elasticity and the engineering approximations for beams, plates, and shells. A finite element model of a free, undamped structure yields the matrix equation

$$M\ddot{\mathbf{u}} + K\mathbf{u} = 0, \tag{1}$$

where M and K are the structural mass and stiffness matrices, respectively, and $\mathbf{u}$ is the vector of displacement components. The compressible fluid is modeled mathematically as a medium for which the pressure satisfies (in the time domain) the scalar wave equation (Zienkiewicz and Newton, 1969)

$$\nabla^2 p = \ddot{p}/c^2, \tag{2}$$

where c is the speed of sound in the fluid. At the fluid-structure interface, momentum and continuity considerations require that the fluid pressure be applied to the structure and that the normal derivative of pressure be proportional to normal acceleration. Thus,

$$\partial p/\partial n = -\rho \ddot{\mathbf{u}}_n, \tag{3}$$

where n is the outward normal (from the structure into the fluid) at the interface, and ρ is the mass density of the fluid. Two numerical approaches are considered in treating the fluid domain: finite element and boundary element.

Finite Element Approach. Since the scalar wave equation (2) is a special case of the vector wave equation satisfied by the structural displacements, the fluid domain can be modeled with the same types of elastic finite elements used to model the

structure if an analogy is drawn between structural displacement and fluid pressure (Everstine, 1981a, 1982; Shin and Chargin, 1983). Thus, if finite elements are used to model both structure and fluid, the system of coupled equations which results is of the form

$$\begin{bmatrix} M & 0 \\ -\rho L^T & Q \end{bmatrix} \begin{Bmatrix} \ddot{\mathbf{u}} \\ \ddot{\mathbf{p}} \end{Bmatrix} + \begin{bmatrix} 0 & 0 \\ 0 & C \end{bmatrix} \begin{Bmatrix} \dot{\mathbf{u}} \\ \dot{\mathbf{p}} \end{Bmatrix} + \begin{bmatrix} K & L \\ 0 & H \end{bmatrix} \begin{Bmatrix} \mathbf{u} \\ \mathbf{p} \end{Bmatrix} = \begin{Bmatrix} 0 \\ 0 \end{Bmatrix}, \tag{4}$$

where $\mathbf{p}$ is the vector of fluid pressures at the fluid grid points, Q and H are the fluid counterparts to the structural mass and stiffness matrices, respectively, $-L$ is the rectangular area matrix which converts a vector of fluid pressures (positive in compression) at the wet structural points to a vector of forces at all points in the output coordinate systems selected by the user, and C is a radiation boundary condition matrix with nonzero entries only for fluid degrees of freedom (DOF) on the outer boundary. A useful alternative to this nonsymmetric system is the symmetric potential formulation (Everstine, 1981b), which is obtained by transforming from fluid pressure $\mathbf{p}$ to fluid velocity potential $\mathbf{q}$ (the time integral of pressure) as the fundamental fluid unknown:

$$\begin{bmatrix} M & 0 \\ 0 & Q \end{bmatrix} \begin{Bmatrix} \ddot{\mathbf{u}} \\ \ddot{\mathbf{q}} \end{Bmatrix} + \begin{bmatrix} 0 & L \\ L^T & C \end{bmatrix} \begin{Bmatrix} \dot{\mathbf{u}} \\ \dot{\mathbf{q}} \end{Bmatrix} + \begin{bmatrix} K & 0 \\ 0 & H \end{bmatrix} \begin{Bmatrix} \mathbf{u} \\ \mathbf{q} \end{Bmatrix} = \begin{Bmatrix} 0 \\ 0 \end{Bmatrix}. \tag{5}$$

This formulation is particularly easy to implement using existing capabilities in general purpose finite element structural analysis computer programs. Other symmetrical forms have been suggested by Morand and Ohayon (1979), MacNeal, Citerley, and Chargin (1980), Ohayon and Valid (1984), Sandberg and Goransson (1988), and Felippa (1988). It is probably still an open question as to which approach is the most economical.

To model the fluid with standard elastic finite elements, the z component of displacement is used to represent the velocity potential q, all other DOF are fixed at fluid grid points, and the fluid element "elastic" properties are specified (Everstine, 1982) as

$$G_e = -1/\rho,\ E_e = -10^{20}/\rho,\ \nu_e = \text{unspecified}, \tag{6}$$

where the subscript e is added to emphasize that these are the values entered on input data cards for the elements. Also, under the analogy, the element "mass density" ρ_e specified for the fluid is

$$\rho_e = \begin{cases} 0, & \text{incompressible fluid } (c \to \infty) \\ -1/(\rho c^2), & \text{compressible fluid } (c \text{ finite}). \end{cases} \tag{7}$$

This specification of material properties is required for symmetry of the coefficient matrices in equation (5). [Examination of the coefficients in the material matrix which converts strain to stress in three-dimensional isotropic elasticity would verify that there are no numerical conditioning problems caused by the material properties specified in equation (6)].

For large expanses of exterior fluid, only a small portion of fluid need be modeled (Zienkiewicz and Newton, 1969; Marcus, 1978; Kalinowski and Nebelung, 1981). For an incompressible fluid, in which there can be no acoustic waves, the outer boundary may be located at one or two structural diameters away from the structure and the pressure-release ($p=0$) boundary condition imposed. (As will be seen later, the fluid matrix H must be invertible to compute the fluid added mass matrix; consequently, the rigid outer boundary condition, $\partial \mathbf{p}/\partial n = 0$, should not be used at the outer fluid boundary.) For a compressible fluid, which can have wave motion, there is some empirical evidence (Kalinowski and Nebelung, 1981) that the fluid boundary can be truncated at one or two acoustic wavelengths away from the structure, and dashpots of constant $-A/(\rho c)$ attached between the fluid DOF and ground to absorb (approximately) the outgoing waves, where A is the area assigned to the boundary point. (This is the plane-wave absorbing boundary condition.)

This theoretical description allows for the possibility of fluid compressibility effects, which impose requirements on the fluid mesh size and extent (Kalinowski and Nebelung, 1981) and which require complex eigenanalysis for the solution of equation (4). Since the interest is often in low frequency vibrations, which interest is equivalent to assuming fluid incompressibility, the previous equations are specialized to the case $c \to \infty$. For an incompressible fluid, the matrices Q and C vanish, and the coupled system [equation (4)] simplifies to

$$\begin{bmatrix} M & 0 \\ -\rho L^T & 0 \end{bmatrix} \begin{Bmatrix} \ddot{\mathbf{u}} \\ \ddot{\mathbf{p}} \end{Bmatrix} + \begin{bmatrix} K & L \\ 0 & H \end{bmatrix} \begin{Bmatrix} \mathbf{u} \\ \mathbf{p} \end{Bmatrix} = \begin{Bmatrix} 0 \\ 0 \end{Bmatrix}. \tag{8}$$

An alternative form of equation (8) results if the pressure vector $\mathbf{p}$ is eliminated from this system to yield

$$(M + M_a)\ddot{\mathbf{u}} + K\mathbf{u} = 0, \tag{9}$$

where the symmetric, nonbanded matrix $M_a = \rho L H^{-1} L^T$ is referred to as the added mass matrix.

The low frequency (added mass) vibration problem can thus be solved by use of the symmetric potential formulation [equation (5) with Q and C both zero], the pressure formulation [equation (8)], or the added mass matrix formulation [equation (9)]. Although all three formulations are theoretically equivalent, the last form [equation (9)] has the advantage of being in standard form for a real eigenvalue problem and, moreover, allows the added mass matrix to be calculated using any suitable approach, including boundary elements and finite elements. However, equation (9) has a considerable disadvantage in that matrix bandedness is destroyed, since M_a couples all the wet DOF to each other. If the surrounding fluid domain is modeled with finite elements, the eigenvalue problem can alternatively be solved using equations (5) or (8), which have more DOF than equation (9) but remain banded if the structural and fluid unknowns are properly sequenced. The main distinction between equations (5) and (8) is that the latter involves nonsymmetric coefficient matrices.

Boundary Element Approach. The added mass matrix in equation (9) can also be obtained by boundary element techniques. Since a solution to Laplace's equation is required, the technique of DeRuntz and Geers (1978) would be applicable. We could alternatively compute the added mass matrix by using a boundary element capability for the Helmholtz equation (e.g., Chen and Schweikert, 1963; Wilton, 1978; Everstine, Henderson, Schroeder, and Lipman, 1986; Everstine, Henderson, and Schuetz, 1987; Everstine and Henderson, 1990) in the low frequency limit. We choose the latter approach since the required fluid matrices are readily available in a convenient form.

In the frequency domain, where the time dependence $\exp(i\omega t)$ is suppressed, the basis for such an approach is the Helmholtz surface integral equation satisfied by the fluid pressure $\mathbf{p}$ on the surface S of a submerged structure:

$$\int_S p(\mathbf{x})(\partial D(r)/\partial n)\,dS - \int_S q(\mathbf{x}) D(r)\,dS = p(\mathbf{x}')/2, \tag{10}$$

where $\mathbf{x}'$ is on S, D is the Green's function

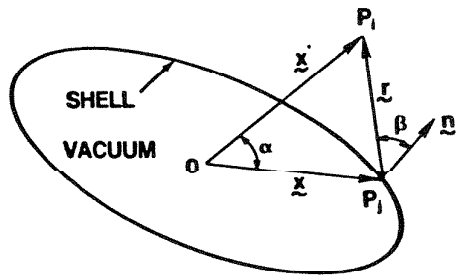

Fig. 1 Notation for Helmholtz integral equation

$$D(r) = e^{-ikr}/4\pi r, \tag{11}$$

$$q = \partial p/\partial n = -i\omega\rho v_n, \tag{12}$$

$k = \omega/c$ is the acoustic wave number, c is the speed of sound in the fluid, r is the distance from $\mathbf{x}$ to $\mathbf{x}'$ (Fig. 1), ρ is the mass density of the fluid, and v_n is the outward normal component of velocity on S. As shown in Fig. 1, $\mathbf{x}$ and $\mathbf{x}'$ in equation (10) are the position vectors for points P_j and P_i on the surface S, the vector $\mathbf{r} = \mathbf{x}' - \mathbf{x}$, and $\mathbf{n}$ is the unit outward normal at P_j. The lengths of the vectors $\mathbf{x}$, $\mathbf{x}'$, and $\mathbf{r}$ are denoted by x, x', and r, respectively. The normal derivative of the Green's function D appearing in equation (10) can be evaluated as

$$\partial D(r)/\partial n = (e^{-ikr}/4\pi r)(ik + 1/r)\cos\beta, \tag{13}$$

where β is defined as the angle between the normal $\mathbf{n}$ and the vector $\mathbf{r}$, as shown in Fig. 1.

The substitution of equations (11)–(13) into the surface equation (10) yields

$$p(\mathbf{x}')/2 - \int_S p(\mathbf{x})(e^{-ikr}/4\pi r)(ik + 1/r)\cos\beta\, dS$$

$$= i\omega\rho \int_S v_n(\mathbf{x})(e^{-ikr}/4\pi r) dS. \tag{14}$$

This integral equation relates the fluid pressure p and normal velocity v_n on S. If equation (14) is discretized for numerical computation (by any of the standard approaches described in the boundary element references cited at the beginning of this section), the matrix equation

$$E\mathbf{p} = C\mathbf{v}_n \tag{15}$$

results on S. The dimensionality of this system (i.e., the dimension of vectors $\mathbf{p}$ and $\mathbf{v}_n$) is f, the number of fluid DOF (the number of wet points on the surface S). Hence, the added mass matrix (the matrix which converts fluid acceleration to fluid force) is, in terms of the fluid DOF,

$$M_n = AE^{-1}C/i\omega, \tag{16}$$

where A is the diagonal $f \times f$ area matrix for the wet surface. As defined in equation (16), M_n is full, symmetric, frequency-dependent, and complex. The low frequency (incompressible fluid) added mass matrix is obtained by evaluating M_n in the limit $\omega \to 0$. Inspection of the integral equation, equation (14), indicates that, for small frequency, E is real and constant, and C is purely imaginary and proportional to ω. Thus, to compute M_n in equation (16), only the real parts of E and $C/i\omega$ for small ω are considered. With this interpretation, the added mass matrix M_n is now full, symmetric, real, and independent of frequency.

To relate the f normal DOF on the wet surface to the complete set of s independent structural DOF, a transformation matrix G is introduced. G is defined as the rectangular $s \times f$ matrix of direction cosines to transform a vector $\mathbf{F}_n$ of outward normal forces at the wet points to a vector $\mathbf{F}$ of forces at all points in the output coordinate systems selected by the user. Thus (Everstine, Henderson, Schroeder, and Lipman, 1986),

$$\mathbf{F} = G\mathbf{F}_n,\ \mathbf{v}_n = G^T\mathbf{v},\ \text{and}\ \mathbf{a}_n = G^T\mathbf{a}, \tag{17}$$

where $\mathbf{v}$ and $\mathbf{a}$ are the velocity and acceleration vectors for the independent structural DOF, respectively, and the subscript n is used to denote the outward normal components of these vectors. For time-harmonic analysis, $\mathbf{v} = i\omega\mathbf{u}$ and $\mathbf{a} = i\omega\mathbf{v}$. The transformation matrix G can then be used to transform the added mass matrix displayed in equation (16) from normal DOF to the independent structural DOF:

$$M_a = GAE^{-1}(C/i\omega)G^T. \tag{18}$$

Here again, only the real parts of E and $C/i\omega$ for small ω are considered. The matrix M_a defined in equation (18) is the boundary element equivalent of the finite element matrix of the same name defined following equation (9). M_a is real, symmetric, nonbanded, and independent of frequency. (The symmetry of M_a, while not obvious from this definition, follows from reciprocity considerations.) The coupling matrix L defined in equation (4) is the product of the transformation and area matrices G and A.

Implementation of the Finite Element Approach

The finite element procedure used here to compute resonances of submerged shells is the symmetric potential formulation as shown in equation (5), except that for incompressible fluids the matrices Q and C are both zero. To solve this system, a finite element model is required for both the structure and a portion of the surrounding fluid. The model for the structure is constructed in the usual way. The model for the fluid domain is constructed using any of the general elastic elements which are geometrically compatible with the elements chosen for the structure. Thus, if the structure is modeled with four-node plates or shells, the fluid should be modeled with eight-node bricks; if the structure is modeled with axisymmetric shell elements, the fluid should be modeled with quadrilateral or triangular axisymmetric ring elements.

Since the z component of displacement represents, by analogy (in both Cartesian and cylindrical coordinate systems), the scalar velocity potential q in equation (5), all other DOF at fluid mesh points are eliminated by constraints. The material properties are assigned to the fluid elements according to equations (6) and (7a). If the fluid is considered to be of infinite extent, the finite element model of the fluid should be truncated not closer than one shell diameter away from the shell, where a pressure-release ($q = 0$) boundary condition is imposed.

The coupling matrix L is entered directly as a symmetric "damping" matrix. L has nonzero entries only at the intersections of matrix columns associated with interface fluid DOF with rows associated with the translational DOF of coincident structural points. Each nonzero entry of L is a component of the outwardly-directed area vector, which is a normal vector whose magnitude is equal to the area assigned to a wet point. Because of the presence of the coupling matrix in the "damping" matrix, the resulting system can then be solved using standard complex eigenvalue analysis techniques, among others. (However, since there is no actual damping, all the natural frequencies are real.)

Implementation of the Boundary Element Approach

The boundary element generation of the added mass matrix is implemented with the fluid matrix generation capability available in the NASHUA structural-acoustics program (Everstine, Henderson, Schroeder, and Lipman, 1986; Everstine, Henderson, and Schuetz, 1987; Everstine and Henderson, 1990). For each unique set of symmetry constraints, the procedure involves two steps, the first of which is

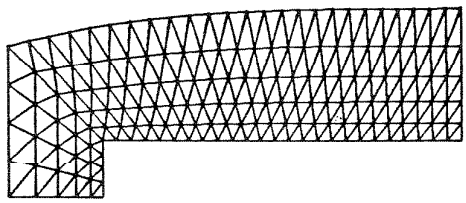

Fig. 2 Axisymmetric finite element model of structure and fluid

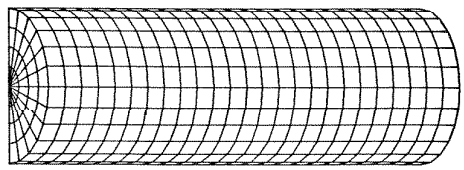

Fig. 3 Finite element model of cylindrical shell

an analysis whose primary purpose is to generate a file containing geometric information and the definition of the wet surface of the structure. The second step involves the sequential execution of a program to generate the matrices G, A, E, and C appearing in equation (18) followed by a finite element analysis for the real eigenvalues. The frequency ω chosen in equation (18) for this analysis is small but nonzero. The nondimensional frequency $ka = 0.01$ is a reasonable choice, where a is a typical length (e.g., radius) of the structure.

Numerical Example

These procedures are illustrated by computing, using both finite element and boundary element techniques, the fluid-loaded resonances of a submerged cylindrical shell with flat end closures. The particular problem solved has the following characteristics:

$a = 5$ m	mean shell radius
$L = 60$ m	shell length
$h = 0.05$ m	shell/end plate thickness
$E = 1.96 \times 10^{11}$ N/m^2	Young's modulus
$\nu = 0.3$	Poisson's ratio
$\rho_s = 7900$ kg/m^3	shell density
$\rho = 1000$ kg/m^3	fluid density
$c = 1500$ m/sec	fluid speed of sound

For the finite element model of both structure and fluid, a half-length model (Fig. 2) was prepared using axisymmetric elements (conical shell for the shell and triangular ring for the fluid). The structural model consisted of 25 elements over the half-length and 4 elements on the end plate. The outer boundary of the fluid model was located about 16 meters from the axis of the shell. Symmetry conditions were imposed at the mid-length, thus restricting the available modes to those symmetric with respect to the mid-length.

For the analysis with added mass effects generated by boundary elements, a general shell model of the structure was prepared using a four-node isoparametric membrane/bending quadrilateral plate element (NASTRAN's QUAD4). A quarter model was prepared (half the length and half the circumference) using 25 elements longitudinally, 12 elements circumferentially, and 4 elements radially on the end plate, as shown in Fig. 3. Symmetry was imposed at both planes of geometric symmetry. Since all fluid effects were computed by the boundary element program, no fluid mesh was required.

Four analyses were performed for this problem:

(*1*) Axisymmetric conical shell model, in-vacuo, circumferential harmonic $n \le 5$, 715 DOF,

(*2*) General plate model, in-vacuo, 2093 DOF,

(*3*) Axisymmetric conical shell model, fluid-loaded, finite element added mass effects, $n \le 5$, 1465 DOF, and

Table 1 In-vacuo and fluid-loaded natural frequencies of cylindrical shell with flat end plates

No.	Mode: Harm. n	Mode: Shell m	Mode: Plate m	Frequency (Hz): Axisym. in-vacuo	Plate in-vacuo	Axisym.subm. (F.E. mass)	Plate subm. (B.E. mass)	Approx. Theory
1	1	0		0	0	0	0	0
2	2	1		2.72	2.72	1.13	1.13	1.11
3	3	1		3.84	3.90	1.79	1.81	1.77
4	0		1	4.27	4.22	1.63	1.44	1.38
5	4	1		7.04	7.19	3.61	3.67	3.57
6	4	3		9.29	9.34	4.81	4.82	4.70
7	1		1	9.53	9.20	4.44	4.26	4.22
8	3	3		10.4	10.4	4.94	4.93	4.82
9	5	1		11.3	11.4	6.31	6.38	6.18
10	5	3		12.2	12.4	6.83	6.86	6.67
11	1	3		13.4	13.3	7.04	6.88	
12	2		1	15.6	15.1	8.31	8.02	
13	5	5		15.8	15.9	8.99	8.88	8.65
14	0		2	15.9	16.4	8.66	8.40	
15	4	5		17.0	16.9	8.94	8.85	8.66
16	2	3	3	18.6	18.5	8.05	8.07	7.75
17	3		1	22.7	22.4	13.2	13.0	
18	5	7		22.9	22.8	13.2	12.9	12.6
19	3	5		24.3	24.1	11.9	11.9	11.5
20	1		2	26.6	27.2	15.4	15.5	
21	4	7		28.4	28.2	15.3	15.1	14.7

(*4*) General plate model, fluid-loaded, boundary element added mass effects, 2093 DOF, final mass matrix not banded.

The first 21 natural frequencies and mode shapes were found among those which have circumferential index $n \le 5$ and are symmetric with respect to the mid-length plane. The results of these calculations are shown in the table. The second column in the table (Harm. n) gives the circumferential harmonic index, the number of full waves around the circumference. (For the end plate, n thus denotes the number of nodal diameters.) The third column (Shell m) gives the number of longitudinal half waves. The fourth column (Plate m) gives the number of nodal circles (plus one) in the end plate. The next two columns of the table list the in-vacuo natural frequencies (in Hz.) of the cylindrical shell for both the conical shell and plate models. The next two columns of the table list the fluid-loaded (fully submerged) resonances of the shell using both models. The added mass effects were computed for the conical shell and plate models using the finite element and boundary element techniques, respectively, as previously described.

The last column of the table lists approximate theoretical predictions for the fluid-loaded resonances. These values were computed in the following way. In general, since frequency is inversely proportional to the square root of mass, the ratio of submerged to in-vacuo resonant frequencies for a structure is

$$f_{\text{wet}}/f_{\text{dry}} = (1 + M_a/M)^{-1/2}, \tag{19}$$

where M_a and M are the added mass and structural mass, respectively. For both plates and cylindrical shells, this ratio of added to structural mass can be written in the form (Junger and Feit, 1986; Blevins, 1979)

$$M_a/M = \alpha(\rho/\rho_s)(a/h), \tag{20}$$

where α is a dimensionless parameter which depends on the boundary conditions, modal wavenumbers, and, for a cylinder, the length-to-radius ratio. For a finite length, simply supported cylindrical shell, α can be approximated for the lobar ($n > 1$) modes as (Junger and Feit, 1986)

$$\alpha = n^2/((n^2+1)(n^2+(m\pi a/L)^2)^{1/2}). \quad (21)$$

For a clamped circular plate, $\alpha = 0.6689$ for the (0,1) mode and 0.3087 for the (1,1) mode, where the two mode numbers indicate, respectively, the number of nodal diameters and the number of nodal circles plus one (Blevins, 1979). Since the conditions under which these relations apply are approximately satisfied with this example, their predictions are included in the table for reference. The ratio [equation (19)] is applied in the table to the average of the two in-vacuo predictions.

As indicated in the table, most of these 21 modes are predominantly shell modes or end plate modes. For one mode (Number 16 in the table), the shell and end plate are both active participants in the modal behavior (although with varying levels of relative participation, depending on the model and whether there was fluid loading).

The results in the table show good general agreement between the predictions of the two approaches, both in-vacuo and fluid-loaded, even for circumferential harmonics 4 and 5. For these two harmonics, the plate mesh has only 6 and 4.8 elements per wavelength, respectively, in the circumferential direction, but still does surprisingly well. The two numerical approaches show agreement within approximately 2 percent for all the fluid-loaded modes which exhibit predominantly shell behavior. The two fluid-loaded predictions for the end plate modes agree within approximately 4 percent of each other, with the exception of Mode 4, the fundamental drum head mode of the plate, where the difference is about 12 percent. In view of the similarity of the boundary element prediction to the approximate theoretical prediction, the boundary element result is probably the better of the two numerical predictions, perhaps indicating that the finite element mesh used (Fig. 2) needs to be extended farther out at the end of the structure.

Discussion

The results presented in the preceding section indicate that both the finite element and boundary element procedures are capable of computing accurate added mass effects due to fluid loading on fully submerged structures. Of the two approaches, the boundary element procedure is the easier to use, since it is highly automated and does not require the generation of a fluid mesh. Even general purpose automatic mesh generators cannot completely solve the fluid meshing issue, since they cannot generate the fluid-structure interface condition, which requires direct matrix input of surface areas. On the other hand, the finite element procedure is somewhat more general, since it can also treat structures which are near other boundaries or are partially submerged (Marcus, 1978).

The computer times required for the two submerged vibration analyses cannot be directly compared, since one analysis used an axisymmetric model, and the other a quarter-model of a general three-dimensional mesh. However, it is possible to make some general projections about efficiencies based on the orders and wavefronts of the various matrices which would be generated by otherwise comparable models. For structures similar to the cylindrical shell considered here, it would appear that the finite element procedure is computationally less expensive than the boundary element procedure. This difference would be due primarily to the exploitation by the finite element method of the banded matrices which occur with long, slender structures. Consider, for example, the plate model of the cylindrical shell shown in Fig. 3. The in-vacuo model had 2093 independent DOF with an average matrix wavefront of 79. When the (boundary element) added mass matrix was combined with the structural mass matrix, the average wavefront increased nearly fivefold to 394. With the eigensolution time proportional to the product of the order of the matrix and the square of the wavefront, the solution time for the submerged case increases by a factor of about 25. On the other hand, for the same structural model, a finite element model of a portion of the surrounding fluid would typically double both the matrix order and the matrix wavefront (compared to the in-vacuo case) since each structural grid point (with six DOF) would require about six fluid grid points (each with one DOF) to be added to the model. Such a model would therefore cost only about eight times as much to run as the "dry" model. The trade-off between the finite element and boundary element procedures for solving the underwater vibration problem thus reduces to a trade-off of engineering time with computer time.

It is concluded therefore that both the finite element and boundary element procedures are capable of computing the fluid loading effects needed for underwater resonance calculations. The more elegant boundary element approach is easier to use but may be more expensive computationally.

References

Blevins, R. D., 1979, *Formulas for Natural Frequency and Mode Shape*, Van Nostrand Reinhold Company, New York.

Chen, L. H., and Schweikert, D. G., 1963, "Sound Radiation from an Arbitrary Body," *J. Acoust. Soc. Amer.*, Vol. 35, pp. 1626–1632.

DeRuntz, J. A., and Geers, T. L., 1978, "Added Mass Computation by the Boundary Element Method," *Int. J. Numer. Meth. in Engrg.*, Vol. 12, pp. 531–549.

Everstine, G. C., 1981a, "Structural Analogies for Scalar Field Problems," *Int. J. Numer. Meth. in Engrg.*, Vol. 17, pp. 471–476.

Everstine, G. C., 1981b, "A Symmetric Potential Formulation for Fluid-Structure Interaction," *J. Sound and Vibration*, Vol. 79, pp. 157–160.

Everstine, G. C., 1982, "Structural-Acoustic Finite Element Analysis, with Application to Scattering," *Proc. 6th Invitational Symposium on the Unification of Finite Elements, Finite Differences, and Calculus of Variations*, H. Kardestuncer, ed., Univ. of Connecticut, Storrs, Connecticut, pp. 101–122.

Everstine, G. C., Henderson, F. M., Schroeder, E. A., and Lipman, R. R., 1986, "A General Low Frequency Acoustic Radiation Capability for NASTRAN," *Fourteenth NASTRAN Users' Colloquium*, NASA CP-2419, National Aeronautics and Space Administration, Washington, D.C., pp. 293–310.

Everstine, G. C., Henderson, F. M., and Schuetz, L. S., 1987, "Coupled NASTRAN/Boundary Element Formulation for Acoustic Scattering," NASA CP-2481, *Fifteenth NASTRAN Users' Colloquim* (National Aeronautics and Space Administration), Washington, D.C., pp. 250–265.

Everstine, G. C., and Henderson, F. M., 1990, "Coupled Finite Element/Boundary Element Approach for Fluid-Structure Interaction," *J. Acoust. Soc. Amer.*, Vol. 87, pp. 1938–1947.

Felippa, C. A., 1988, "Symmetrization of Coupled Eigenproblems by Eigenvector Augmentation," *Comm. Appl. Numer. Meth.*, Vol. 4, pp. 552–563.

Geers, T. L., 1971, "Residual Potential and Approximate Methods for Three-Dimensional Fluid-Structure Interaction Problems," *J. Acoust. Soc. Amer.*, Vol. 49, pp. 1505–1510.

Junger, M. C., and Feit, D., 1986, *Sound, Structures, and Their Interaction*, 2nd ed., The MIT Press, Cambridge, Massachusetts.

Kalinowski, A. J., and Nebelung, C. W., 1981, "Media-Structure Interaction Computations Employing Frequency Dependent Mesh Sizes with the Finite Element Method," *The Shock and Vibration Bulletin*, Vol. 51, Part 1, pp. 173–193.

MacNeal, R. H., Citerley, R., and Chargin, M., 1980, "A Symmetric Modal Formulation of Fluid-Structure Interaction, Including a Static Approximation to Higher Order Modes," Paper 80-C2/PVP-116, American Society of Mechanical Engineers, New York.

Marcus, M. S., 1978, "A Finite-Element Method Applied to the Vibration of Submerged Plates," *J. Ship Research*, Vol. 22, pp. 94–99.

Morand, H., and Ohayon, R., 1979, "Substructure Variational Analysis of the Vibrations of Coupled Fluid-Structure Systems. Finite Element Results," *Inter. J. Numer. Meth. in Engrg.*, Vol. 14, pp. 741–755.

Ohayon, R., and Valid, R., 1984, "True Symmetric Variational Formulations for Fluid-Structure Interaction in Bounded Domains—Finite Element Results," in *Numerical Methods in Coupled Systems*, edited by R. W. Lewis, P. Bettess, and E. Hinton, John Wiley and Sons Ltd, London, pp. 293–325.

Sandberg, G., and Goransson, P., 1988, "A Symmetric Finite Element Formulation for Acoustic Fluid Structure Interaction Analysis," *J. Sound and Vibration*, Vol. 123, pp. 507–515.

Shin, Y. S., and Chargin, M. K., 1983, "Acoustic Responses of Coupled Fluid-Structure System by Acoustic-Structural Analogy," *The Shock and Vibration Bulletin*, Vol. 53, Part 2, pp. 11–21.

Wilton, D. T., 1978, "Acoustic Radiation and Scattering From Elastic Structures," *Int. J. Numer. Meth. in Engrg.*, Vol. 13, pp. 123–138.

Zienkiewicz, O. C., and Newton, R. E., 1969, "Coupled Vibrations of a Structure Submerged in a Compressible Fluid," *Proceedings of the International Symposium on Finite Element Techniques*, Stuttgart, pp. 359–369.